Structural Studies of a Family of High Affinity Ligands for GPIIb/IIIa

Alvin C. Bach, II,*,⊥ Charles J. Eyermann,⊥ John D. Gross,†,⊥ Michael J. Bower,‡,⊥ Richard L. Harlow,§ Patrica C. Weber,⊥ and William F. DeGrado⊥

Contribution from the Dupont Merck Pharmaceutical Company, Experimental Station, Box 80336, Wilmington, Delaware 19880-0336, and Central Research & Development Department, E. I. du Pont de Nemours and Company, P.O. Box 80228, Wilmington, Delaware 19880-0228

Received September 20, 1993®

Abstract: A class of potent orally active cyclic peptide antagonists of the glycoprotein IIb/IIIa adhesion molecule have been prepared by linking a tetrapeptide, RGD-containing sequence between the two ends of a semirigid linker, *m*-(aminomethyl)benzoic acid (Mamb). To determine how this amino acid constrains the conformation of the intervening peptide sequence and to shed some light on the receptor-bound conformation of the peptide, we examined the solution and solid-state structures of nine cyclic analogues whose receptor binding constants span approximately 4 orders of magnitude. The general structure of these analogues is *cyclo*(Xxx-Arg-Gly-Asp-Mamb). The backbone conformations of each compound trace out a rectangular shape with a β-turn centered at the Xxx-Arg bond. In the most potent compounds in this series Xxx is a small, aliphatic D-amino acid, and N^{α} of the Arg residue is methylated: peptides containing these features are highly rigid and contain a type II′ β-turn centered at the D-Abu-*N*-MeArg dipeptide, a highly extended Gly residue, and a C_7 turn centered at the Asp. Peptides lacking the *N*-methyl group and/or with reversed chirality at Xxx are more flexible. The N^{α}-methyl group also restricts the conformation of the Arg side chain. In addition the aliphatic side chain of the D-amino acid, the N^{α}-methyl of *N*-MeArg, and the phenyl group of the Mamb linker form a continuous hydrophobic surface, which presumably interacts favorably with the receptor. Finally, the effects of conformational constraints introduced at the Mamb and the Asp residues were investigated to determine their effects on receptor binding.

Introduction

The discovery and optimization of peptides capable of binding to biological receptor molecules is an activity of fundamental interest to the field of molecular recognition and practical interest to the pharmaceutical industry. In recent years, several biological and chemical approaches have been developed to prepare and sort through vast libraries of peptides in search of compounds with high affinity for a receptor of interest.[1-4] One potential drawback of this approach is that peptides are highly flexible molecules, and hence it is difficult to define their biologically active conformation and lock them into this state. One way to partially overcome this limitation is to prepare libraries of disulfide cross-linked peptides[5] or to embed the random sequences within the tertiary structure of a protein[6] of known structure, although the resulting peptides still retain a large degree of flexibility. Therefore, we have begun to develop new approaches to the solid-phase synthesis of highly conformationally constrained peptides for use in compound libraries.

In a previous communication, we described template constrained cyclic peptides, in which one introduces a semirigid template into a cyclic peptide.[7] The template is intended to limit the conformational flexibility of the intervening peptide sequence. This strategy was evaluated with impressive results using the Arg-Gly-Asp (RGD) sequence as a test case. Linear peptides containing this tripeptide bind to the receptor, IIb/IIIa, with about 10 μM dissociation constants, whereas cyclic RGD-containing peptides that incorporated the template, *m*-(aminomethyl)benzoic acid, bound with considerably higher affinity (up to 100 pM). A systematic set of analogues were prepared to determine the features that gave rise to this high affinity (Figure 1). The most tight binding compound were *cyclo*(D-Abu-*N*-MeArg-Gly-Asp-Mamb) (**1**) and *cyclo*(D-Val-*N*-MeArg-Gly-Asp-Mamb) (**2**) where D-Abu is α-aminobutyric acid and *N*-MeArg is N^{α}-methylarginine. The D-chirality of the amino acid at position 1 of the sequence and the *N*-methylation of the Arg were found to be particularly important for obtaining high binding affinity. Additional conformationl constraints that were compatible with high activity (but did not necessarily lead to tighter binding) included the introduction of a phenyl ring onto the methylene group of the Mamb or the addition of a methyl group onto the β-methylene of the Asp residue. In these cases, two isomers were prepared, and one was shown to be considerably more active than the other.

In the present paper, we examine a number of different peptides (Figure 1) to determine the extent to which each of these features influence the conformation of the peptide. These peptides include compounds **1-3**, all of which are highly active and have a D-amino acid (D-Abu, D-Val, or D-Ala, respectively) at position 1 and *N*-MeArg at position 2. To assess the role of the *N*-methyl group, *cyclo*(D-Abu-Arg-Gly-Asp-Mamb) (**4**) has also been examined. Further, comparison of this compound with *cyclo*(Ala-Arg-Gly-Asp-Mamb) (**5**), which has L-Ala at position 1, helps to define the effect of the first chiral center. Finally, comparison of the two isomers of the C^{β}-methyl-Asp-containing peptides (**6** and **7**), and the two isomers of the phenyl-Mamb derivatives (**8** and **9**)

† Present address: Department of Chemistry, Massachusetts Institute of Technology, Cambridge, MA.

‡ Present address: Department of Pharmaceutical Chemistry, University of California at San Francisco, San Francisco, CA.

§ E. I. DuPont de Nemours, Wilmington, DE.

⊥ Dupont Merck Pharmaceutical Co.

® Abstract published in *Advance ACS Abstracts*, February 15, 1994.

(1) Lam, K. S.; Salmon, S. E.; Hersh, E. M.; Hruby, V. J.; Kazmierski, W. M.; Knapp, R. J. *Nature* **1991**, *354*, 82-84.

(2) Cwirla, S. E.; Peters, E. A.; Barrett, R. W.; Dower, W. J. *Proc. Natl. Acad. Sci. U.S.A.* **1990**, *87*, 6378-6382.

(3) Devlin, J. J.; Ranganiban, L. C.; Devlin, P. E. *Science* **1990**, *249*, 404-406.

(4) Houghton, R. A.; Pinilla, C.; Blondelle, S. E.; Appel, J. R.; Dooley, C. T.; Cuervo, J. H. *Nature* **1991**, *354*, 84-86.

(5) O'Neil, K. T.; Hoess, R. H.; Jackson, S. A.; Ramachandran, N. S.; Mousa, S. A.; DeGrado, W. F. *Proteins* **1992**, *14*, 509-515.

(6) O'Neil, K. T.; DeGrado, W. F.; Hoess, R. H. in *Techniques in Protein Chemistry V*; Academic Press: Orlando, FL, in press.

(7) Jackson, S. A.; Harlow, R. L.; Dwivedi, A.; Parthasarathy, A.; Higley, A. C.; Krywko, J.; Rockwell, A.; Markwalder, J. A.; Wells, G. J.; Mousa, S. A.; DeGrado, W. F. *J. Am. Chem. Soc.*, following paper in this issue.

0002-7863/94/1516-3207$04.50/0

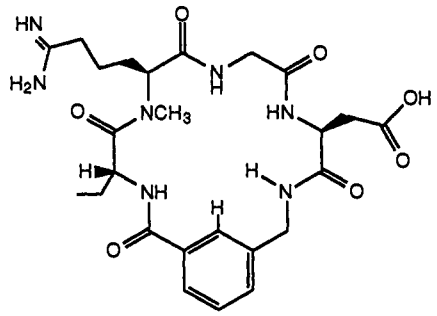

1 *cyclo*(D-Abu-N-MeArg-Gly-Asp-Mamb)

2 *cyclo*(D-Val-N-MeArg-Gly-Asp-Mamb)

3 *cyclo*(D-Ala-N-MeArg-Gly-Asp-Mamb)

4 *cyclo*(D-Abu-Arg-Gly-Asp-Mamb)

5 *cyclo*(Ala-Arg-Gly-Asp-Mamb)

6 *cyclo*(D-Val-N-MeArg-Gly-β-Me-Asp-Mamb) Isomer 1

7 *cyclo*(D-Val-N-MeArg-Gly-β-Me-Asp-Mamb) Isomer 2

8 *cyclo*(D-Val-N-MeArg-Gly-Asp-α-phenyl-Mamb) Isomer 1

9 *cyclo*(D-Val-N-MeArg-Gly-Asp-α-phenyl-Mamb) Isomer 2

Figure 1. Chemical formula of *cyclo*(D-Abu-*N*-MeArg-Gly-Asp-Mamb) (**1**) and the sequences of the other cyclic peptides in this study. The proton at the two position of the phenyl ring is indicated.

have allowed us to better define the receptor-bound conformation of these peptides.

Methods

NMR Methods. NMR experiments were performed at 499.8 MHz on a Varian VXR-500S spectrometer. NMR samples were prepared under dry nitrogen gas in 0.8 mL of 99.996% DMSO-d_6 (Merck) at the concentrations listed in the table and figure captions. TMS (1 μL) was used as an internal chemical shift reference. Spectra in D_2O were referenced to the HOD peak at 4.79 ppm at 25 °C. A 1.5-s relaxation delay was used in all experiments.

One-dimensional FT experiments were collected with 16 384 complex points. For variable-temperature experiments, the sample was allowed to equilibrate in the probe for 30 min before data collection.

DQF-COSY,[8,9] TOCSY,[10,11] and ROESY[12,13] two-dimensional spectra were recorded. TOCSY data sets were recorded using the clean-TOCSY pulse sequence with 35–50 ms spin locking times and 1-ms trim pulses. ROESY spectra were recorded with a 3.0 KHz spin locking field using the method of Kessler.[14] RF compensation was achieved using the method of Dezheng.[15] For each sample, data at several spin locking times in the range 50–300 ms were recorded.

Two-dimensional experiments were obtained with spectral widths of either 5800 or 7000 Hz in both dimensions. Complex points (2048) were collected in t2, and 256 complex points were collected in t1. Transients (32 or 64) were coadded for each t1 value. All spectra were acquired in the phase-sensitive absorption mode with quadrature detection in both dimensions.[16,17]

Two-dimensional data sets were processed using the FELIX program (Biosym Inc.). Matrix files were 1024 × 1024 points in size. All t2 time domain transforms were weighted with a skewed sine bell, shifted 80 degrees, with a skew factor of 1.1. The t1 interferograms were also weighted with the same apodization function of the appropriate length. In most cases a high-order polynomial was then applied to flatten the baseline in both dimensions. Most ROESY data sets were collected with the t1 delay set to the calculated value of the second point in the interferogram.[18] The first point was back-calculated before transformation using the linear predication routine built into FELIX. In the other cases, the first point of each interferogram was multiplied by 0.5 before transformation to eliminate t1 artifacts.[19]

Proton chemical shifts assignments were made using standard techniques.[20]

ROE (rotating frame nuclear Overhauser effect) crosspeak volumes were measured using FELIX software. These were converted to interproton distances using the ROE between the two H^β protons of *N*-MeArg or Arg as a standard distance which was set to 1.8 Å. The calculated distances were independent of spin locking time between 50 and 300 ms. The spin locking times used for each calculation are listed below. ROE data beyond C^β was not used in structure calculation.

Computational Methods. Conformations consistent with the NMR data were generated based on well-established procedures.[21-23] For compounds **1**, **4**, and **5**, 500 ROE-constrained conformations were generated using the distance geometry program DGEOM (available from QCPE, Department of Chemistry, Indiana University, Bloomington, IN 47405). *Cis*-amide bonds were allowed, and no distance correlation was used in the distance sampling. Lower-bound distance constraints were set to 20% less than the derived interproton distance, and upper bounds were set to 30% greater than this value. Antidistance constraints (ADCs) corresponding to interproton distances which did not produce an observed ROE were assigned a lower bound of 3 Å.[24] Distance constraints were applied using a square-well potential with a 50 kcal mol^{-1} Å^{-2} force constant applied outside the lower and upper bounds. Chiral constraints were applied to all chiral and prochiral centers. ROEs involving methyl protons were represented as distances to the methyl carbon.

The Gly H^α protons were stereochemically assigned using $J^{N\alpha}$ coupling constants and a transannular ROE between the Mamb H2 ring proton and one of the Gly H^α resonances (see Figure 2). The conformational calculations described below were run in parallel, with the assignment of the transannular ROE switched between the Gly *pro-R* and *pro-S* H^α protons. The chirality of the Gly C^α was fixed in all distance geometry calculations.

Constrained minimization of the initial distance geometry structures was done using the TRIPOS force field[25] without including electrostatic terms. The *N*-MeArg(Arg) and Asp side chains were kept neutral. Conformations with a distance constraint energy of 2 kcal/mol or less were then minimized with ROE constraints and electrostatic terms calculated using partial atomic charges based on the Gasteiger–Marsili method.[26-28] Those conformations with constraint energies of 2 kcal/mol or less and a total energy within 15 kcal of the lowest energy conformer were finally checked for consistency with all the NMR data, including $J^{N\alpha}$ coupling constants using the equation of Bystrov.[29] Conformations which did not have ROE errors greater than 0.5 Å and which had ϕ angles within 30 degrees of the allowed values calculated from $J^{N\alpha}$ coupling constants were taken as viable NMR solution conformations. Clustering

(8) Piantini, U.; Sorensen, O. W.; Ernst, R. R. *J. Am. Chem. Soc.* **1982**, *104*, 6800–6801.
(9) Shaka, A. J.; Freeman, R. *J. Magn. Reson.* **1983**, *51*, 169–173.
(10) Davis, D. G.; Bax, A. *J. Am. Chem. Soc.* **1985**, *107*, 2820–2821.
(11) Griesinger, C.; Otting, G.; Wuethrich, K.; Ernst, R. R. *J. Am. Chem. Soc.* **1988**, *110*, 7870–7872.
(12) Bothner-By, A. A.; Stephens, R. L.; Lee, J.; Warren, C. D.; Jeanloz, R. W. *J. Am. Chem. Soc.* **1984**, *106*, 811–813.
(13) Bax, A.; Davis, D. G. *J. Magn. Reson.* **1985**, *63*, 207–213.
(14) Kessler, H.; Griesinger, C.; Kerssebaum, R.; Wagner, K.; Ernst, R. R. *J. Am. Chem. Soc.* **1987**, *109*, 607–609.
(15) Dezheng, Z.; Fujiwara, T.; Nagayama, K. *J. Magn. Reson.* **1989**, *81*, 628–630.
(16) Müller, L.; Ernst, R. R. *Mol. Phys.* **1979**, *38*, 963–992.
(17) States, D. J.; Haberkorn, R. A.; Ruben, D. J. *J. Magn. Reson.* **1982**, *48*, 286–292.
(18) Marion, D.; Bax, A. *J. Magn. Reson.* **1989**, *83*, 205–211.
(19) Otting, G.; Widmer, H.; Wagner, G.; Wuethrich, K. *J. Magn. Reson.* **1986**, *66*, 187–193.
(20) Wüthrich, K.; Billeter, M.; Braun, W. *J. Mol. Biol.* **1984**, *180*, 715–740.
(21) Peishoff, C. E.; Bean, J. W.; Kopple, K. D. *J. Am. Chem. Soc.* **1991**, *113*, 4416–4421.
(22) Peishoff, C. E.; Ali, F. E.; Bean, J. W.; Calvo, R.; D'Ambrosio, C. A.; Eggleston, D. S.; Hwang, S. M.; Kline, T. P.; Koster, P. F.; Nichols, A.; Powers, D.; Romoff, T.; Samanen, J. M.; Stadel, J.; Vasko, J. A.; Kopple, K. D. *J. Med. Chem.* **1992**, *35*, 3962–3969.
(23) Kopple, K. D.; Baures, P. W.; Beans, J. W.; D'Ambrosio, C. A.; Hughes, J. L.; Peishoff, C. E.; Eggleston, D. S. *J. Am. Chem. Soc.* **1992**, *114*, 9615–9623.
(24) Brüschweiler, R.; Blackledge, M.; Ernst, R. R. *J. Biomol. NMR* **1991**, *1*, 3–11.
(25) Clark, M.; Cramer, R. D., III; Opdenbosch, N. V. J. *J. Comput. Chem.* **1989**, *10*, 892–1012.
(26) Gasteiger, J.; Marsili, M. *Tetrahedron* **1980**, *36*, 3219–3228.
(27) Marsili, M.; Gasteiger, J. *Croat. Chem. Acta* **1980**, *53*, 601–614.
(28) Gasteiger, J.; Marsili, M. *Org. Magn. Reson.* **1981**, *15*, 353–360.
(29) Bystrov, V. F.; Portnova, S. L.; Bahashova, T. A.; Koz'min, S. A.; Gavrilov, Y. D.; Afanas'ev, V. A. *Pure Appl. Chem.* **1973**, *36*, 19–34.

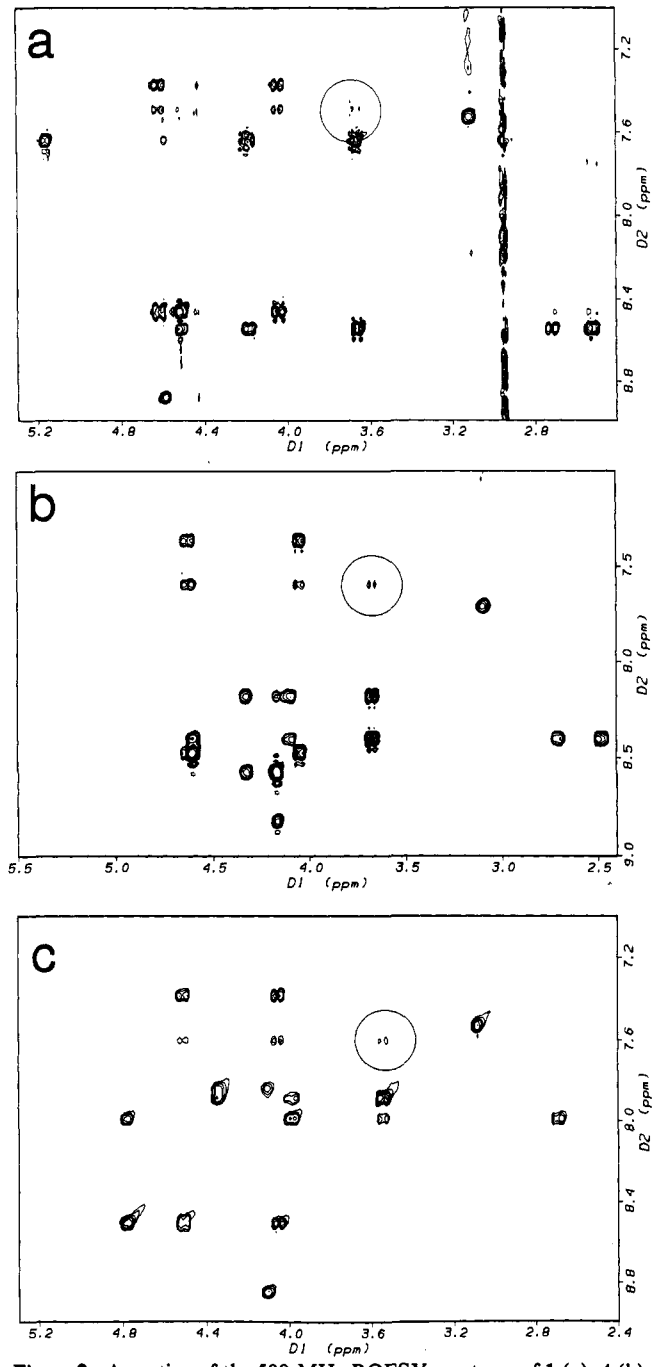

Figure 2. A portion of the 500-MHz ROESY spectrum of **1** (a), **4** (b), and **5** (c), showing the transannular ROE between the Mamb H2 proton and the *pro-S* Gly H^{α} proton (circled).

of the final conformations into structural families was done based on RMS differences in the X-Xxx-Arg-Gly-Asp backbone conformations.

Determination of Gly Stereochemistry. For **1**, when the ROE between Mamb H2 ring proton and one of the Gly H^{α} resonances is assigned to the *pro-S* H^{α}, the resulting single family of conformations have Gly ϕ values between −112° and −162°. Such a range would produce $J^{N\alpha}$ values between 6.4 and 10.7 Hz for the *pro-R* and 1.0–3.2 Hz for the *pro-S* protons.[29] Reversing the assignment also produces one conformational family. The Gly ϕ values are between 70° and 83°, corresponding to $J^{N\alpha}$ values between 7.2 and 8.3 Hz for the *pro-R* and 5.3–7.4 Hz for the *pro-S* protons. Given the experimentally observed values of 8.1 and 3.0 Hz, we assigned the ROE to the *pro-S* H^{α} proton.

The same procedure was followed for **4**, where two families of conformers resulted from the calculations using the initial *pro-S* Gly H^{α} assignment: The first has Gly ϕ values between −155° and −162°, corresponding to $J^{N\alpha}$ values between 6.4 and 7.5 Hz for the *pro-R* proton and between 0.6 and 1.0 Hz for the *pro-S* proton. The second family has Gly ϕ values between −131° and −137°, corresponding to $J^{N\alpha}$ values between 10.0 and 10.5 Hz for the *pro-R* proton and between 0.6 and 1.0 Hz for the *pro-S* proton.

Table 1. NOE-Derived Distance Constrants for *cyclo*(D-Abu-*N*-MeArg-Gly-Asp-Mamb) **1** in DMSO-d_6 at 25 °C (150 ms Mix)

from		to		calcd distance	lower bound	upper bound
D-Abu	NH	Mamb	H2	2.9	2.3	3.7
D-Abu	NH	Mamb	H6	2.3	1.8	3.0
Gly	NH	Mamb	H2	2.7	2.2	3.5
Gly	NH	Nmr[a]	Me	2.5	2.0	3.2
Gly	NH	Nmr	H^{α}	2.5	2.0	3.2
Asp	NH	Gly	$H^{\alpha 1}$	2.2	1.8	2.9
Asp	NH	Gly	$H^{\alpha 2}$	2.5	2.0	3.3
Asp	NH	Asp	$H^{\beta 1}$ [b]	2.4	1.9	3.1
Asp	NH	Asp	$H^{\beta 2}$ [b]	2.6	2.1	3.4
Mamb	NH	Asp	H^{α}	2.1	1.7	2.8
Mamb	NH	Mamb	H2	2.6	2.1	3.4
Mamb	H2	Asp	H^{α}	3.2	2.5	4.1
Mamb	H2	Nmr	Me	3.6	2.9	4.7
Mamb	H2	Gly	$H^{\alpha 1}$	3.1	2.5	4.0
Mamb	H2	Mamb	$H^{\alpha 2}$ [b]	2.7	2.2	3.5
Mamb	H2	Mamb	$H^{\alpha 1}$ [b]	2.8	2.2	3.6
Mamb	H4	Mamb	$H^{\alpha 1}$ [b]	2.5	2.0	3.3
Mamb	H4	Mamb	$H^{\alpha 2}$ [b]	2.5	2.0	3.3

[a] Nmr-*N*-MeArg. [b] Numerals indicate nondegenerate resonances but do not imply prochirality.

When the Gly Hα *pro-R* assignment is used in calculating conformations of **4**, three families of conformers result. The first has Gly ϕ values between 65° and 75°, corresponding to $J^{N\alpha}$ values between 6.5 and 6.8 Hz for the *pro-R* and between 5.0 and 5.9 Hz for the *pro-S* protons. The second conformational family has Gly ϕ values between 49° and 56°, corresponding to $J^{N\alpha}$ values between 6.7 and 6.8 Hz for the *pro-R* and between 3.0 and 3.8 Hz for the *pro-S* protons. The third family has Gly ϕ values between 150° and 160°, corresponding to $J^{N\alpha}$ values between 0.4 and 1.0 Hz for the *pro-R* proton and between 6.8 and 8.4 Hz for the *pro-S* proton. The experimentally observed values of 8.3 and 3.5 for **4** agree best with the ROE assigned to *pro-S* H^{α} proton.

For compound **5**, the two Gly $J^{N\alpha}$ coupling constant values are too close in value, making this type of analysis invalid. They were therefore assigned based on chemical shift, assuming the more upfield shifted proton was *S*, as in **1** and **4**.

The accurate determination of the solution conformation of **1**, **4**, and **5** is predicated on the correct stereochemical assignment of the Gly H^{α} protons. In the recent work on small RGD peptides the sterochemical assignment of the Gly H^{α} protons has always been reported as being ambiguous.[22,23,30,31] In our study, the presence of a consistently observable transannular ROE (see Figure 2) and extreme $J^{N\alpha}$ values for the Gly NH enables the assignment of the *pro-S* proton as closest to the H2 proton of the Mamb residue across the backbone ring (see Figure 1).

For **1**, only one conformational family was obtained with the reversed stereochemical assignment, which has Gly ϕ values inconsistent with the observed coupling constants. For **4**, three families are obtained under the same reversed assignment; two are completely inconsistent with the observed values. The range of $J^{N\alpha}$'s found for the third family places the experimentally observed $J^{N\alpha}$'s at the edge of the range and is unlikely to be correct.

Structure Generation of 1, 4, and 5. To determine the solution structure of **1**, a total of 18 distance constraints were derived from a 150-ms ROESY 2D spectrum of **1** (Table 1). An additional 85 ADCs (antidistance constraints) with a 3.0 Å lower bound were also included in the calculations to generate the initial 500 conformations. A total of 172 conformations passed the 2 Kcal fixed distance range energy test of the first constrained minimization; 121 of these conformers passed another 2 Kcal fixed distance range energy test of the second constrained minimization, and 119 were within the lowest 15 Kcals of energy.

These 119 conformers were tested against consistent ϕ values (±30°) calculated from the $J^{N\alpha}$ coupling constants (see Table 2). The D-Abu ϕ was constrained to be near 70°, 170°, −20°, or −100°. The Gly ϕ was constrained to be near ±135°. The Asp ϕ was constrained to be near 38°, 81°, −85°, or −155°.

A total of 38 conformers satisfied all four $J^{N\alpha}$ constraints, containing no distance constraint violations greater than 0.1 Å. These 38 conformers were within 0.48 Å RMS difference of each other and clustered into one conformational family for **1**, based on the X-R-G-D backbone.

Table 2. Proton Chemical Shifts of *cyclo*(D-Abu-*N*-MeArg-Gly-Asp-Mamb) **1** (6.9 mM) in DMSO-d_6 at 25 °C

residue	HN[a]	$\Delta\delta/\Delta T$[b]	H$^{\alpha a}$	H$^{\beta a}$	H$^{\gamma a}$	other[a]	$J^{N\alpha}$[c]
D-Abu	8.88	−6.6	4.60	1.77	0.95		5.1
N-MeArg	2.95 (Me)		5.15	1.58/2.02	1.35	H$^{\delta}$: 3.11	
						ϵNH: 7.53	
Gly	7.64	−4.0	3.66^S/4.18^R				8.1, 3.0
Asp	8.55	−3.9	4.51	2.51/2.71			7.5
Mamb	8.46	−5.5	4.04/4.62			H2: 7.48	7.5, 5.0
						H4: 7.37	
						H5: 7.37	
						H6: 7.71	

[a] PPM. [b] ppb/deg. [c] Hz.

Table 3. NOE-Derived Distance Constrants for *cyclo*(D-Abu-Arg-Gly-Asp-Mamb) **4** in DMSO-d_6 at 25 °C (200 ms Mix)

from		to		calcd distance	lower bound	upper bound
D-Abu	NH	Mamb	H2	2.6	2.0	3.3
D-Abu	NH	Mamb	H4	2.2	1.8	2.9
D-Abu	NH	D-Abu	H$^{\alpha}$	2.6	2.1	3.4
Arg	NH	Mamb	H2	3.7	2.9	4.8
Arg	NH	Mamb	H2	2.5	2.0	3.2
Arg	NH	D-Abu	H$^{\alpha}$	2.0	1.6	2.6
Arg	NH	Arg	H$^{\beta 1\,a}$	2.3	1.9	3.0
Gly	NH	Mamb	H2	3.0	2.4	3.9
Gly	NH	D-Abu	H$^{\alpha}$	3.4	2.7	4.5
Gly	NH	Arg	H$^{\alpha}$	2.7	2.2	3.5
Asp	NH	Mamb	H2	3.2	2.6	4.2
Asp	NH	Gly	H$^{\alpha 2}$	2.7	2.1	3.5
Asp	NH	Gly	H$^{\alpha 1}$	2.2	1.8	2.9
Asp	NH	Asp	H$^{\beta 1\,a}$	2.5	2.0	3.2
Asp	NH	Asp	H$^{\beta 2\,a}$	2.7	2.2	3.5
Mamb	NH	Mam	H2	2.4	1.9	3.2
Mamb	H2	Gly	H$^{\alpha 1}$	2.8	2.2	3.6
Mamb	H2	Mamb	H$^{\alpha 1\,a}$	3.2	2.5	4.1
Mamb	H2	Mamb	H$^{\alpha 2\,a}$	2.8	2.3	3.7
Mamb	H4	Mamb	H$^{\alpha 2\,a}$	2.6	2.1	3.4
Mamb	H4	Mamb	H$^{\alpha 1\,a}$	2.4	2.0	3.2

[a] Numerals indicate nondegenerate resonances but do not imply prochirality.

Table 4. Proton Chemical Shifts of *cyclo*(D-Abu-Arg-Gly-Asp-Mamb) (23.3 mM) **4** in DMSO-d_6 at 25 °C

residue	HN[a]	$\Delta\delta/\Delta T$[b]	Hα[a]	H$^{\beta\,a}$	H$^{\gamma\,a}$	other[a]	$J^{N\alpha}$[c]
D-Abu	8.83	−6.4	4.17	1.77	0.92		6.4
Arg	8.58	−5.6	4.33	1.48/2.03	1.48	H$^{\delta}$: 3.11	9.2
						ϵNH: 7.71	
Gly	8.19	−3.5	3.69^S/4.10^R				8.3, 3.5
Asp	8.41	−3.8	4.60	2.48/2.71			8.0
Mamb	8.48	−5.8	4.06/4.62			H2: 7.60	7.7, 4.8
						H4: 7.36	
						H5: 7.36	
						H6: 7.66	

[a] PPM. [b] ppb/deg. [c] Hz.

For determining the structure of **4**, a total of 21 distance constraints were derived from a 200-ms ROESY 2D spectrum (Table 3). An additional 86 ADCs with a 3.0 Å lower bound were also included in the calculations to generate the initial 500 conformations. A total of 190 conformers passed the 2 Kcal fixed distance range energy test of the first constrained minimization; 128 of these conformations passed the 2 Kcal fixed distance range energy test of the second constrained minimization all of which were within 15 Kcals of each other.

The 128 conformers were tested against consistent ϕ values (±30°) calculated from the $J^{N\alpha}$ coupling constants (see Table 4).[29] The D-Abu ϕ was constrained to be near 78°, 162°, −30°, or −90°. The Arg ϕ was constrained to be near −96° or −144°. The Gly ϕ was constrained to be near ±130°. The Asp ϕ was constrained to be near 45°, 76°, −87°, or −153°.

A total of 46 conformers satisfied the five $J^{N\alpha}$ constraints, which were all within 0.20 Å RMS difference of each other. They clustered into two conformational families, based on the X-R-G-D backbone.

Table 5. NOE-Derived Distance Constrants for *cyclo*(L-Ala-Arg-Gly-Asp-Mamb) **5** in DMSO-d_6 at 25 °C (200 ms Mix)

from		to		calcd distance	lower bound	upper bound
Ala	NH	Arg	NH	2.7	2.1	3.5
Ala	NH	Mamb	H6	2.1	1.7	2.8
Ala	HH	Ala	Hβ	2.4	2.0	3.2
Arg	NH	Ala	H$^{\alpha}$	2.8	2.2	3.6
Arg	NH	Arg	H$^{\beta 1\,a}$	4.1	3.3	5.4
Gly	NH	Arg	H$^{\alpha}$	2.5	2.0	3.2
Gly	NH	Mamb	H2	3.0	2.4	3.9
Gly	NH	Ala	H$^{\alpha}$	3.5	2.8	4.6
Asp	NH	Mamb	H2	3.2	2.6	4.2
Asp	NH	Gly	H$^{\alpha 1}$	2.4	2.0	3.2
Asp	NH	Gly	H$^{\alpha 2}$	3.1	2.5	4.1
Asp	NH	Asp	H$^{\beta 1\,a}$	2.8	2.3	3.7
Asp	NH	Asp	H$^{\beta 2\,a}$	2.8	2.2	3.6
Asp	NH	Mamb	H2	2.7	2.2	3.5
Mamb	NH	Asp	NH	3.3	2.7	4.3
Mamb	NH	Asp	H$^{\alpha}$	2.1	1.7	2.8
Mamb	NH	Mamb	H2	2.3	1.9	3.1
Mamb	H2	Gly	H$^{\alpha 1}$	3.1	2.5	4.1
Mamb	H2	Mamb	H$^{\alpha 1\,a}$	3.0	2.4	3.9
Mamb	H2	Mamb	H$^{\alpha 2\,a}$	2.8	2.2	3.7
Mamb	H4	Mamb	H$^{\alpha 1\,a}$	2.3	1.8	2.9
Mamb	H4	Mamb	H$^{\alpha 2\,a}$	2.6	2.1	3.4

[a] Numerals indicate nondegenerate resonances but do not imply prochirality.

Table 6. Proton Chemical Shifts of *cyclo*(L-Ala-Arg-Gly-Asp-Mamb) (17.8 mM) **5** in DMSO-d_6 at 25 °C

residue	HN[a]	$\Delta\delta/\Delta T$[b]	H$^{\alpha\,a}$	H$^{\beta\,a}$	H$^{\gamma\,a}$	other[a]	$J^{N\alpha}$[c]
L-Ala	8.87	−7.4	4.11	1.42			4.8
Arg	7.86	−2.0	4.34	1.45/1.98	1.37	H$^{\delta}$: 3.09	9.2
						ϵNH: 7.59	
Gly	7.90	−1.2	3.53^S/3.99^R				6.8, 4.9
Asp	8.01	−0.9	4.79	2.27/2.70			8.7
Mamb	8.51	−6.4	4.06/4.52			H2: 7.61	7.0, 5.4
						H4: 7.39	
						H5: 7.38	
						H6: 7.66	

[a] PPM. [b] ppb/deg. [c] Hz.

The solution structures of **5** determined from 22 distance constraints were derived from a 200-ms ROESY 2D spectrum (Table 5). An additional 201 ADCs with a 3.0 Å lower bound were also included in the calculations to generate the initial 500 conformations. A total of 348 conformers passed the 2 Kcal fixed distance range energy test of the first constrained minimization; 128 of these conformers passed the 2 Kcal fixed distance range energy test of the second constrained minimization, and 322 were within the lowest 15 Kcals of energy.

The 328 conformers were tested against consistent ϕ values (±30°) calculated from the $J^{N\alpha}$ coupling constants (see Table 6).[29] The L-Ala ϕ was constrained to be near 18°, 101°, −68°, or −171°. The Arg ϕ was constrained to be near −96° or −144°. The Gly ϕ was constrained to be near ±131° and ±58°. Further tightening of the Gly ϕ constraint was not possible because the two Gly $J^{N\alpha}$'s are too similar to each other. The Asp ϕ was constrained to be near 60°, −93°, or −148°.

Seventy conformers satisfied all five $J^{N\alpha}$ constraints and clustered into four conformational families which were within 1.38 Å RMS difference

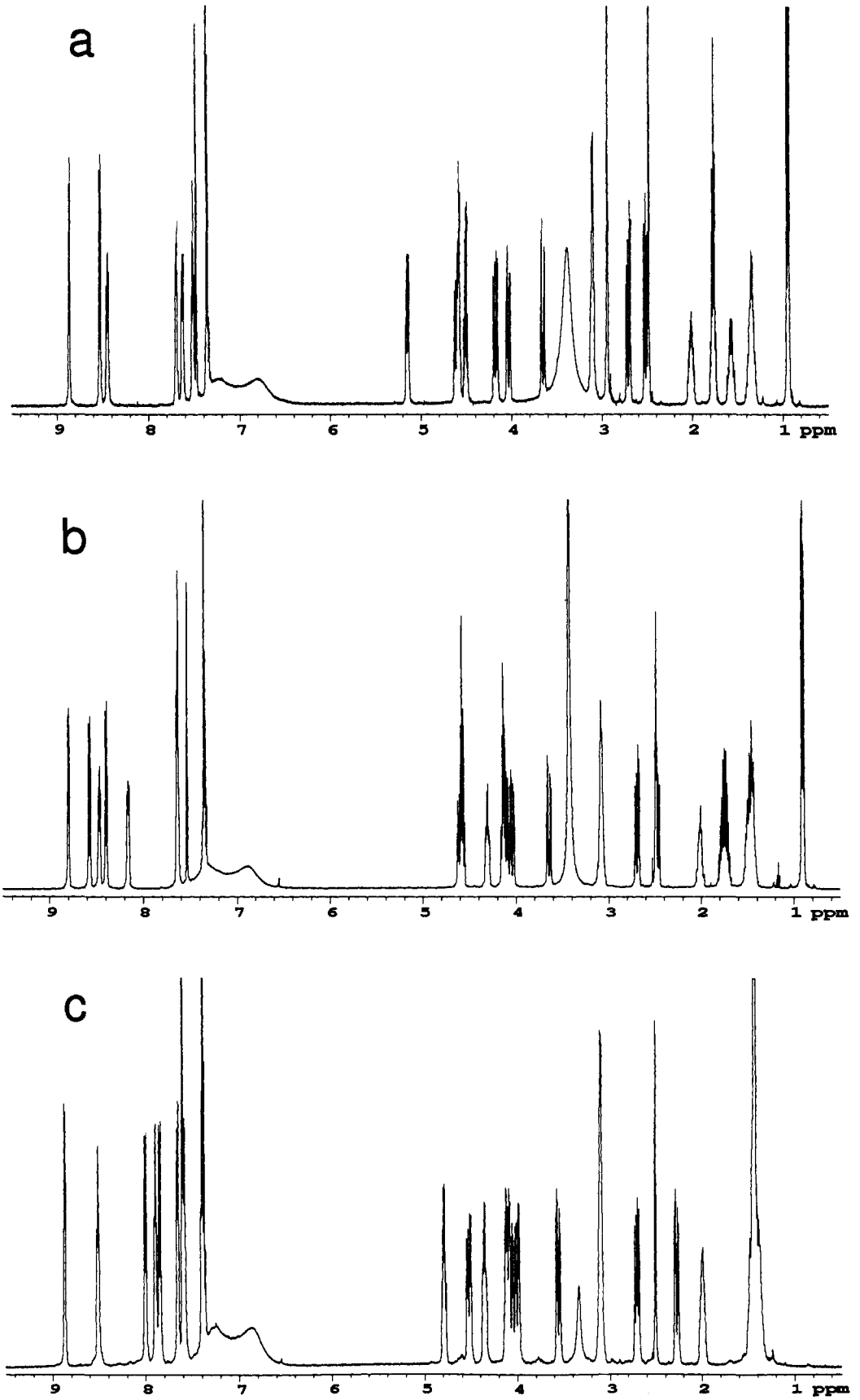

Figure 3. 500-MHz ^{1}H NMR spectra of **1** (a), **4** (b), and **5** (c) all in DMSO-d_6 at 25 °C. Sample concentrations: **1**, 6.9 mM; **4**, 23.3 mM; **5**, 17.8 mM. All three spectra show dispersed amide and H^{α} protons.

of each other, based on the X-R-G-D backbone. Two are extended and two are bent at the Gly residue. The bent conformations cannot be ruled out because the two observed Gly $J^{N\alpha}$ values are not as different from each other as they are in **1** and **4** (see Tables 2, 4, and 6).

Results and Discussion

General NMR. Compounds **1**, **4**, and **5** all give single-component spectra with no indication of slow conformational

Table 7. Proton Chemical Shifts of *cyclo*(D-Val-*N*-MeArg-Gly-β-Me-Asp-Mamb) **6** (8.5 mM) in DMSO-d_6 at 25 °C

residue	HN[a]	$\Delta\delta/\Delta T$[b]	$H^{\alpha a}$	$H^{\beta a}$	$H^{\gamma a}$	other[a]	$J^{N\alpha}$ [c]	$J^{\alpha\beta}$ [c]
D-Val	9.00	−7.3	4.35	2.13	0.95/1.14		5.5	
N-MeArg	3.00 (Me)		5.22	1.58/2.06	1.38	H^{δ}: 3.15		
						εNH: 7.56		
Gly	7.68	−4.5	3.64/4.36				9.5, 2.7	
β-Me-Asp	8.52	−5.1	4.40	2.83		β-Me: 1.14	8.5	9.7
Mamb	8.38	−6.1	4.02/4.71			H2: 7.43	7.9, 4.6	
						H4: 7.38		
						H5: 7.38		
						H6: 7.67		

[a] PPM. [b] ppb/deg. [c] Hz.

Table 8. Proton Chemical Shifts of *cyclo*(D-Val-*N*-MeArg-Gly-β-Me-Asp-Mamb) **7** (8.0 mM) in DMSO-d_6 at 25 °C

residue	HN[a]	$\Delta\delta/\Delta T$[b]	$H^{\alpha a}$	$H^{\beta a}$	$H\gamma^a$	other[a]	$J^{N\alpha}$ [c]	$J^{\alpha\beta}$ [c]
D-Val	9.00	−7.4	4.30	2.13	0.94/1.11		5.6	
N-MeArg	3.02 (Me)		5.20	1.59/2.07	1.38	H^{δ}: 3.13		
						εNH: 7.56		
Gly	7.62	−3.6	3.60/4.25				8.5, 2.3	
β-Me-Asp	8.50	−5.2	4.41	2.71		β-Me: 1.09	8.2	10.7
Mamb	8.70	−6.2	4.01/4.70			H2: 7.41	7.5, 4.9	
						H4: 7.38		
						H5: 7.38		
						H6: 7.67		

[a] PPM. [b] ppb/deg. [c] Hz.

Table 9. Proton Chemical Shifts of *cyclo*(D-Val-*N*-MeArg-Gly-Asp-α-Ph-Mamb) **8** (16.4 mM) in DMSO-d_6 at 25 °C

residue	HN[a]	$H^{\alpha a}$	$H^{\beta a}$	$H^{\gamma a}$	other[a]	$J^{N\alpha}$ [b]
D-Val	8.99	4.39	2.16	0.95/1.12		6.2
N-MeArg	3.01 (Me)	5.21	1.60/2.08	1.38	H^{δ}: 3.14	
					εNH: 7.61	
Gly	7.67	3.63/4.23				8.3, 3.2
Asp	8.65	4.68	2.51/2.71			7.5
α-Ph-Mamb	8.64	6.10			H2: 7.71	8.6
					H4: 6.96	
					H5: 7.30	
					H6: 7.63	
					Ph-*o*: 7.30	
					Ph-*m*: 7.37	
					Ph-*p*: 7.37	

[a] PPM. [b] Hz.

averaging near room temperature (Figure 3). Each was easily assigned using standard NMR techniques. There is no evidence for *cis*-peptide bonds in any of these compounds, or the other six compounds examined, as judged by the lack of H^{α} to H^{α} ROEs.

Several NMR parameters point to the presence of a predominant, stable solution conformation or a family of rapidly interconverting, highly similar conformations of all seven compounds in DMSO-d_6. First, the amide proton resonances are well dispersed with maximum chemical shift differences ($\Delta\delta$) of 0.64 ppm in **1** and 4 to 1.56 ppm in **9** (see Tables 2, 4, and 6–10). Second, the $J^{N\alpha}$ coupling constants show a range of values which are stable between 25 °C and 65 °C. Particularly striking are the extreme $J^{N\alpha}$ coupling constant values for the Gly and Mamb NH resonances. Such values are strong indicators for a preferred solution conformation.[32] Third, there are sizable variations in the amide $\Delta\delta/\Delta T$ values, indicating that all the amide protons are not in the same averaged environment. Finally, the two diasterotopic Gly H^{α} proton resonances have $\Delta\delta$'s ranging from 0.41 (in **4**) to 0.72 ppm (in **6**, see Tables 2, 4, and 6–10), again indicating that the methylene protons are not in an averaged environment in solution.[32] The two Mamb methylene proton resonances are similarly dispersed with values of $\Delta\delta$ from 0.46 ppm in **5** to 0.69 ppm in **6**.

(30) Bogusky, M. J.; Naylor, A. M.; Pitzenberger, S. M.; Nutt, R. F.; Brady, S. F.; Colton, C. D.; Sisko, J. T.; Anderson, P. S.; Veber, D. F. *Int. J. Peptide Protein Res.* **1992**, *39*, 63–76.

(31) McDowell, R. S.; Gadek, T. R. *J. Am. Chem. Soc.* **1992**, *114*, 9245–9253.

(32) Kessler, H. *Angew. Chem., Int. Ed. Engl.* **1982**, *21*, 512–523.

The preference toward a single conformation is also seen in H_2O. Two related cyclic peptides, **2**, *cyclo*(D-Val-*N*-MeArg-Gly-Asp-Mamb), and **3**, *cyclo*(D-Ala-*N*-MeArg-Gly-Asp-Mamb), exhibit nearly identical $J^{N\alpha}$ coupling constants in both DMSO-d_6 and H_2O (Table 11). The data in Table 11 are nearly identical to the $J^{N\alpha}$ coupling contants for **1**, **4**, **5**, **6**, **7**, **8**, and **9** in DMSO-d_6 (see Tables 2, 4, and 6–10). Conformational analyses of **2** and **3** in DMSO-d_6 (data not shown) clearly show that they adopt solution conformations similar to those observed for **1**, **4**, and **5** (see below).

These strong indicators for a preferred conformation are also consistent with several X-ray crystal structures of **1** where different crystal forms all give rise to essentially the same peptide backbone conformation in the solid state (see below).

Solution Conformation of *cyclo*(D-Abu-*N*-MeArg-Gly-Asp-Mamb), 1. The solution conformation of **1** was determined as described in the Experimental Section. A striking feature of **1** is that it appears to adopt a single conformation in solution. Examination of ϕ, ψ plots (Figure 4) for 38 distance geometry generated structures of **1** show that these angles fall within very narrow regions of the map, suggesting the presence of narrow and well-defined energy wells. Furthermore, the orientation of the Arg side chain appears to be reasonably well-defined up to the C^{δ} atom as assessed from the fact that χ_1 and χ_2 values lie almost exclusively within one of the two regions of the plot, centered at −180°, −180°, and −50°, −180°.

The predominant solution structure (Figure 5 and Table 12) is similar to classical cyclic hexapeptides which have an overall

Table 10. Proton Chemical Shifts of *cyclo*(D-Val-*N*-MeArg-Gly-Asp-α-Ph-Mamb) **9** (16.4 mM) in DMSO-d_6 at 25 °C

residue	HN[a]	$H^{\alpha a}$	$H^{\beta a}$	$H^{\gamma a}$	other[a]	$J^{N\alpha}$ [b]
D-Val	9.11	4.37	2.22	0.94/1.12		6.1
N-MeArg	3.11 (Me)	5.20	1.60/2.08	1.36	H^{δ}: 3.13	
					εNH: 7.62	
Gly	7.55	3.83/4.26				8.6, 2.8
Asp	8.16	4.31	2.54/2.63			6.8
α-Ph-Mamb	8.65	6.20			H2: 7.82	9.1
					H4: 7.37	
					H5: 7.37	
					H6: 7.85	
					Ph-*o*: 7.16	
					Ph-*m*: 7.31	
					Ph-*p*: 7.24	

[a] PPM. [b] Hz.

Table 11. Comparison of $J^{N\alpha}$ in H_2O and DMSO-d_6 for **2**, *cyclo*(D-Val-*N*-MeArg-Gly-Asp-Mamb), and **3**, *cyclo*(D-Ala-*N*-MeArg-Gly-Asp-Mamb)

	2		**3**	
residue	DMSO-d_6	H_2O	DMSO-d_6	H_2O
2 = *D*-Val	5.9	5.0	5.5	4.6
3 = *D*-Ala				
Gly	Σ = 11.2	Σ = 11.5	Σ = 11.1	Σ = 11.5
Asp	7.5	6.4	7.6	6.8
Mamb	Σ = 12.7	Σ = 12.8	Σ = 12.4	Σ = 12.8

rectangular shape with two connected β-turns.[33] In compound **1**, the first is an almost ideal type II′ β-turn centered at the D-Abu-N-MeArg residues (Table 12). Only the *N*-MeArg ψ is significantly different from the ideal angles for this type of turn.[34] The presence of this turn is supported by the relatively small $\Delta\delta/\Delta T$ value for the Gly NH resonance (see Table 2) and an ROE between the Gly NH and the Mamb H2 protons. The methyl group of the *N*-MeArg residue points up when viewed as in the top panel of Figure 5. Because the Mamb residue lacks appropriate H-bonding functionality, a second β-turn is not found. However, a γ-turn is found at the Asp residue. The Gly residue is generally extended, with the molecule presenting an elongated face between the *N*-MeArg and Asp residues.

The possibility of conformational averaging in **1** could be assessed by comparing the calculated interproton distances (in the distance geometry-generated structures) with those expected from the intensities of the ROEs. The only distance violations were very small (<0.1 Å) and involved the H2 proton of the Mamb aromatic ring and the D-Abu NH or the *pro-S* H^{α} proton of Gly. These appear to arise because the plane of the Mamb is somewhat variable with respect to the peptidic portion of the molecule. Thus, although the peptide portion is conformationally invariant, a limited hinge bending motion is centered at the D-Abu φ, ψ, and the Mamb methylene group. These torsional angles act as a hinge allowing approximately a 140° to 170° angle between the phenyl linker and the rough plane of the peptide, as defined by the C^{α} atoms of D-Abu, *N*-MeArg, Asp, and Mamb residues.

Solution Conformation of *cyclo*(D-Abu-Arg-Gly-Asp-Mamb), 4. Examination of the φ, ψ plots (Figure 4) for **4** show that this peptide is more conformationally variable than **1**; the φ, ψ angles cluster within broader energy wells than for **1**, and the Asp residue samples two regions of the φ, ψ plot. Also, the Arg side chain has four well populated χ_1/χ_2 rotomeric pairs as compared to two for **1**. Two distinct conformational families were observed for **4**, which were again similar to classical double β-turn cyclic hexapeptides and the conformation of **1** (Figure 6). Family *4A* is very similar to *4B*, the largest difference being a 20° change in the orientation of the D-Abu-Arg bond (Table 12). Both of these conformations had substates in which the Asp-Mamb amide bond was flipped by about 180° via a concerted change in the torsional angles centered on the Asp C^{α} and the Mamb methylene groups.

The presence of a type II′ β-turn in **4** is supported by the relatively small $\Delta\delta/\Delta T$ value for the Gly NH resonance. Also, an ROE is seen between the Gly NH and the D-Abu H^{α}, an ROE between the $i+2$ and $i+4$ positions is typically observed in type II′ β-turns.[35] The Asp residue forms an inversed γ-turn and the Gly residue is generally extended.

Again, small (up to 0.13 Å) violations involving the H2 proton of the Mamb aromatic ring are observed for both families, and presumably arise from the hinge bending, which varies from 134° to 137° in **4**. Also observed is a minor violtion in the upper bound distance between the Gly NH and the D-Abu H^{α}.

Solution Conformation of *cyclo*(L-Ala-Arg-Gly-Asp-Mamb), 5. Compound **5** showed a larger degree of conformational ambiguity (Figure 4) than **1** and **4**, which is particularly evident in the smaller differences in Gly $J^{N\alpha}$ coupling constants (Table 6). The Arg χ_1 and χ_2 sidechain dihedral angles show no preferred rotamer in **5**. Cluster analysis indicates that there are four distinct conformations for **5**, shown in Figure 7. Families *5A* and *5D* are similar to families *1*, *4A*, and *4B*, with an extended Gly residues. Families *5B* and *5C* are more bent, having a slight kink at the Gly residue, which results in the Asp residue being positioned above the major plane of the peptide backbone while still maintaining a C7-like turn appearance.

A constant feature between each of the conformational families of **5** is a type I β-turn centered at the Ala-Arg bond. In *5C* this type I turn is near ideal. The presence of this turn is further supported by the low-temperature coefficient of the Gly amide proton and an ROE between the Gly NH and the Ala H^{α} (Table 12), which is characteristic of a type I β-turn.[35] The major differences between the four conformational families for **5** lie within the Gly and Asp residues, which show multiple conformations (Figure 4). Further, the high degree of conformational variability in the Arg side chain is striking when compared to **1**.

The observed violations of the distance constraints for **5** are different from those observed for **1** and **4**. The Gly *pro-S* H^{α} to Mamb H2 constraint is not a major source of error. The predominant violation is a small error in the constraint between Gly NH and Ala H^{α} with no conformer containing an error >0.15 Å.

The hinge bend of the Mamb aromatic ring is more variable in **5** averaging between 150° and 160° in *5A*, *5B*, and *5C*. The bend is less pronounced in *5D* with an average value of 136°.

Effect of Reversing Chirality at the First Position. In compounds **1** and **4**, the D-Abu is in the $i+1$ position of a type II′ β-turn. In **5**, L-Ala is in the $i+1$ position of a type I β-turn, but this chirality change does not alter the observed double β-turn motif. In both turn types, the NH or N^{α}-CH_3 is pointing in the same direction. There is no effect on the dihedral angles of the

(33) Gierasch, L. M.; Deber, C. M.; Madison, V.; Niu, C.-H.; Blout, E. R. *Biochemistry* **1981**, *20*, 4730–4738.
(34) Smith, J. A.; Pease, L. G. *CRC Crit. Rev. Biochem* **1980**, *8*, 315–399.
(35) Wüthrich, K. *NMR of Proteins and Nucleic Acids*; Wiley-Interscience: New York, 1986; pp 126–127.

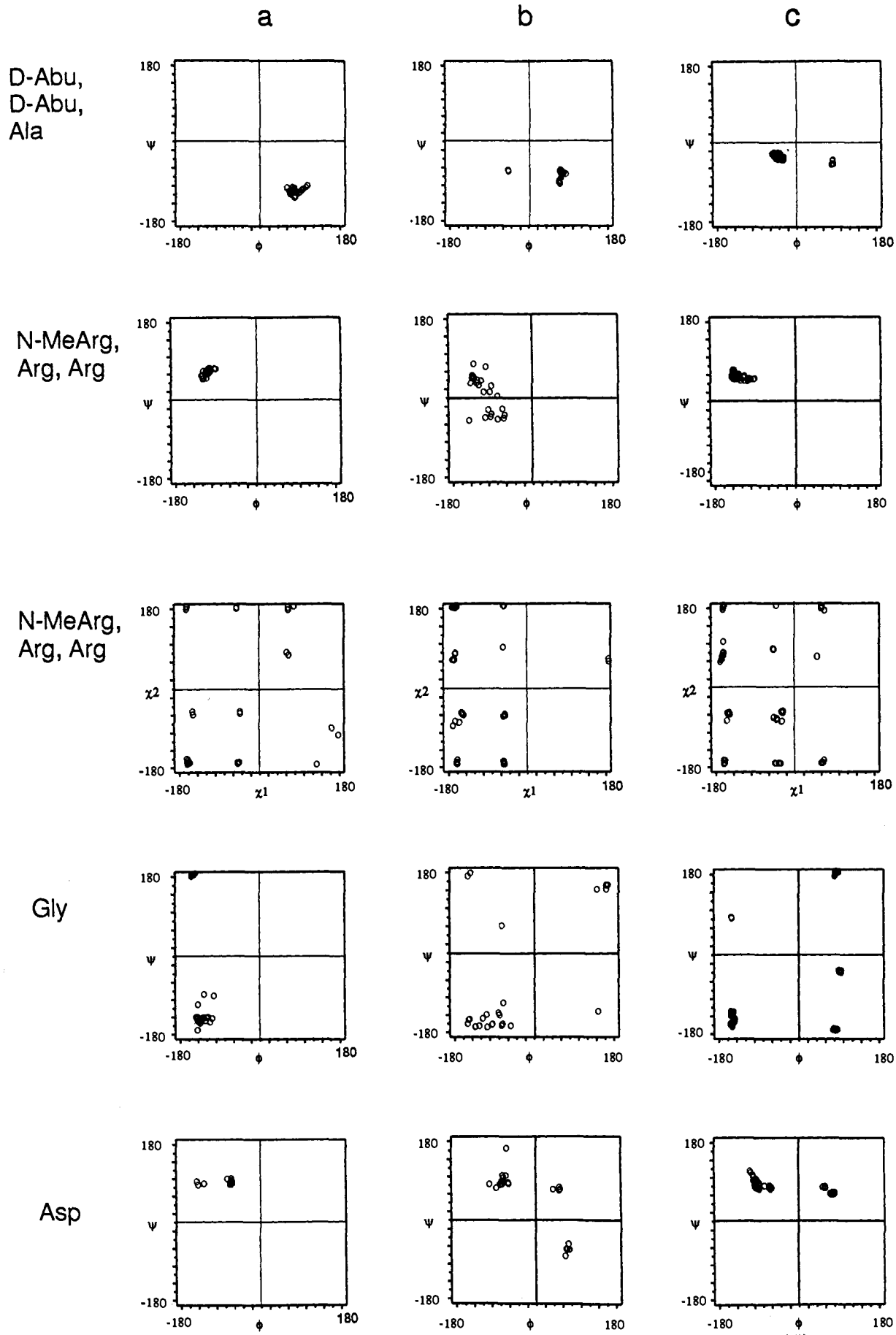

Figure 4. Ramachandran plots for the X-Xxx, Arg(N-MeArg), Gly, and Asp residues and the Arg(N-MeArg) χ_1 versus χ_2 for all the conformers found in the NMR-based structure calculation of **1** (a), **4** (b), and **5** (c). See text for discussion. Note that although the Gly of compound **1** shows two minima (at the bottom and at the top of the ϕ, ψ plot), they are separated by only 20° for ψ and ϕ is the same in both cases.

Table 12. ϕ and ψ Angles from the Centroid Conformations of the NMR-Derived Conformational Families of **1**, **4**, and **5**

	X-Xxx		*N*-MeArg (Arg)		Gly		Asp	
family	ϕ	ψ	ϕ	ψ	ϕ	ψ	ϕ	ψ
1	52	−112	−117	55	−143	−161	−74	94
II′ β-turn	60	−120	−80	0				
4A	65	−73	−146	56	−159	−159	−74	77
4B	60	−99	−120	50	−137	−167	−78	80
5A	−41	−48	−141	56	−155	−162	−97	77
5B	−52	−33	−132	58	71	−176	66	56
5C	−46	−36	−123	50	64	8	−94	62
5D	−51	−43	−146	48	−156	59	49	74
Iβ-turn	−60	−30	−90	0				

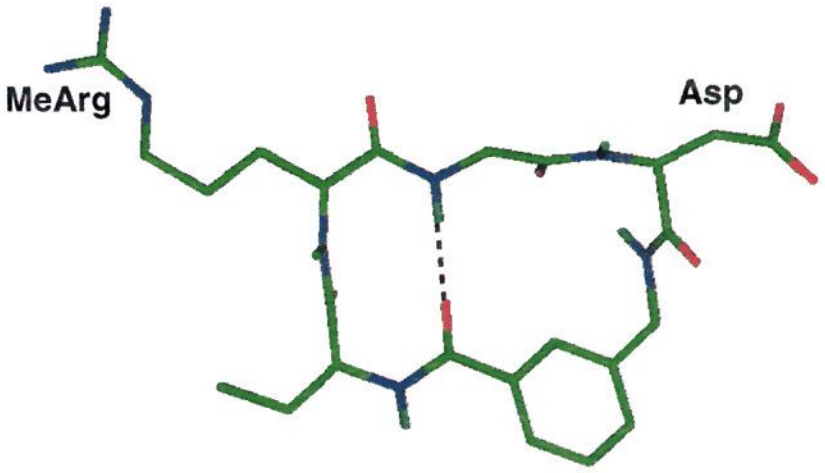

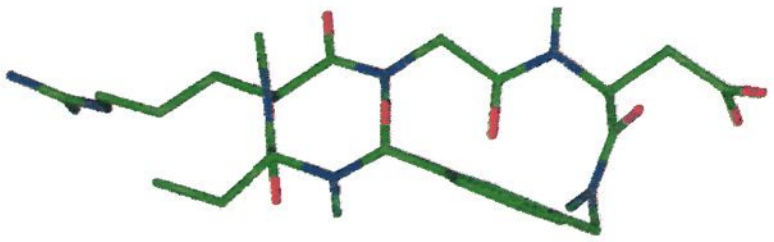

Figure 5. The centroid conformer from the calculated conformational family of **1**. Dihedral angles for this conformer are shown in Table 12. The double β-turn appearance and the flatness of the conformation are clearly visible. The N^{α}-methyl group points up in the top pannel. The H-bond between the Mamb carbonyl and the Gly NH is shown.

N-MeArg or Arg residue. In both cases, the observed ϕ and ψ angles are centered in a region allowed for N-methylated amino acids.[36]

However, the type I turn formed in **5** is not completely conformationally equivalent to the type II′ turn in **1** and **4**. The type I turn has a +45° virtual-bond dihedral angle, formed by the four C^{α}'s and the type II′ has a 0° virtual-bond dihedral angle.[37] Hence, the two turns have different twists to them. In these compounds, the Mamb aromatic C1 is equivalent to the C^{α} atom of an amino acid. In **1** and **4**, the β-turn virtual-bond dihedral angle averages to −25°. In **5**, with its L-Ala, the virtual-bond dihedral angles are in the same range as those for **1** and **4** with the exception of family *5C* which is +25°. This value is much more consistent with the type I turn's natural twist.[37] In the other three conformational families, the cyclic constraints appear to impose the −25° average.

Determination of Stereochemistry of β-Me Asp Analogs by NMR. Racemic C^{β}-methyl Asp was incorporated into an Mamb-containing peptide, *cyclo*(D-Val-*N*-MeArg-Gly-β-Me-Asp-Mamb), giving two isomers (**6** and **7**) which were separated by HPLC. In platelet aggregation assays, **6** has an IC_{50} less than 10^3 less than **7**. We attempted to determine the absolute stereochemistry of **6** and **7** in an attempt to define the biologically active conformation of the Asp side chain.

A comparison of the NMR parameters for **6** and **7** (Tables 7 and 8) with those of **1**, **4**, and **5**, indicates that **6** and **7** most resembles **1**, suggesting that their backbone conformations are very similar.

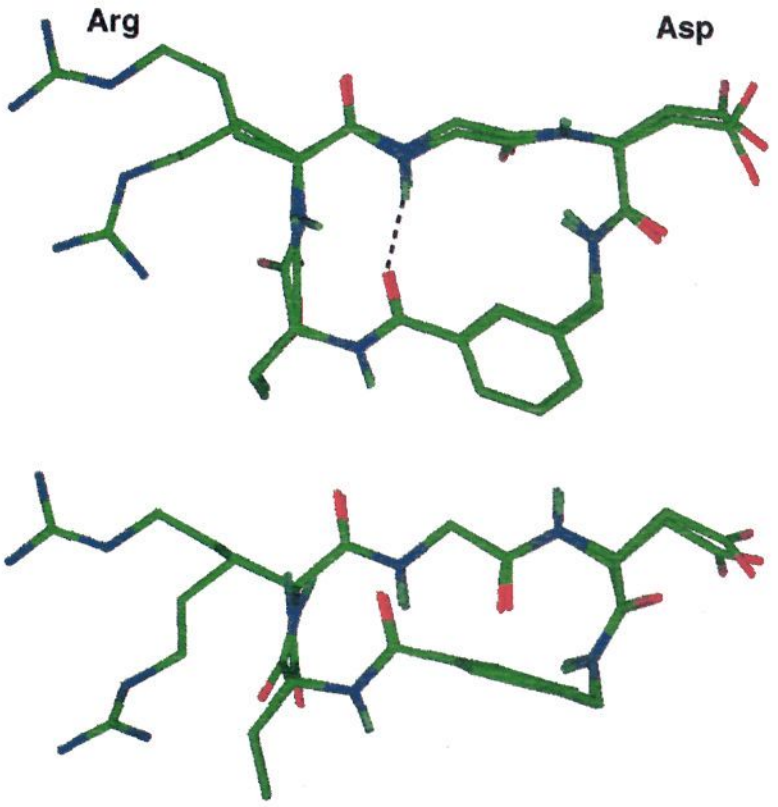

Figure 6. The centroid conformations from each of the two conformational families calculated for **4**. Dihedral angles for these conformers are shown in Table 12. Except for a slight difference in the orientation of the peptide bond between D-Abu and Arg, the two centroid conformations are identical. They are both similar to that observed for **1** (see Figure 5).

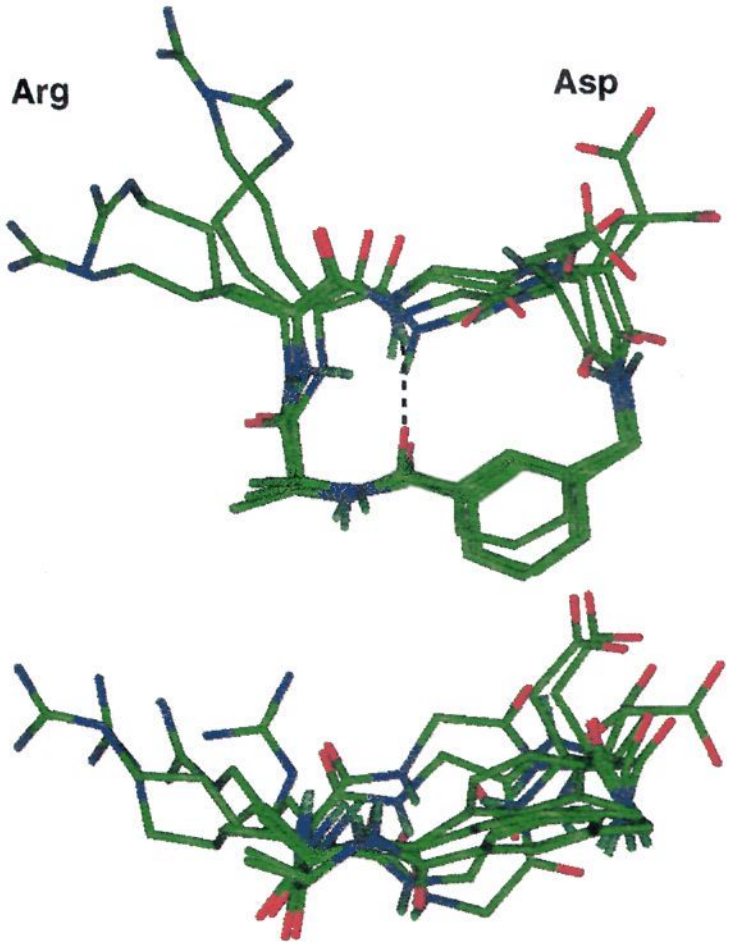

Figure 7. The centroid conformation from each of the four conformational families calculated for **5**. Dihedral angles for these conformers are shown in Table 12. All four centroid conformations maintain a general appearance similar to the double β-turn conformation observed for **1** and **4**, but two of the centroid conformers in **5** are bent.

(36) Manavalan, P.; Momany, F. A. *Biopolymers* **1980**, *20*, 1943–1973.
(37) Richardson, J. B. in *Advances in Protein Chemistry*; Anfinsen, C. B., Edsall, J. T., Richards, F. M.; Eds.; Academic Press: Orlando, 1981; pp 167–339.

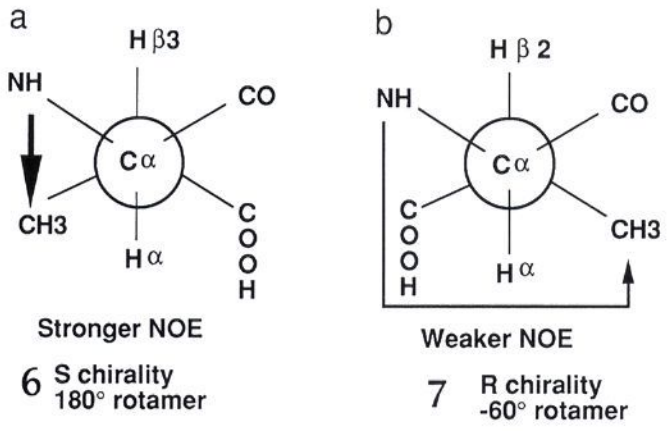

Figure 8. Summary of the ROEs observed in **6** (a) and **7** (a) and a derivation of the stereochemistry of the Asp C^{β}. See text for explanation.

ROESY experiments were used to determine the stereochemistry of the Cβ. To avoid complications from determining which rotamer distributions were present in **6** and **7**, the predominant rotamer for χ_1 was assumed to be the same as that found for the β-branched amino acids Val and Ile in proteins.[38-40] This places the H^{α} and H^{β} protons in an anti orientation, $\chi_1 = 180°$. This assumption was supported by the large $J^{\alpha\beta}$ coupling constants observed for **6** and **7** (Tables 7 and 8).

The chirality of the C^{β}-methyl group in **6** and **7** was determined based on the strength of the ROE between the Asp NH proton resonance and the β-methyl resonance (see Figure 8). This procedure led to the assignment of *R* for **7** and *S* for **6**. These results indicate the more active compound has the carboxylic acid pointing away from the region of the *N*-MeArg residue and strongly suggests that the $GP^{IIb}/^{IIa}$ receptor binds RGD peptides with an Asp $\chi 1$ value of approximately 180°.

Determination of Stereochemistry of α-Phenyl Mamb Analogs. Two diasteromeric α-phenyl Mamb peptides (**8** and **9**) were prepared from racemic α-phenyl Mamb to determine the effect of a chiral substituent at the methylene of the Mamb. In platelet aggregation assays **8** has an IC_{50} two orders of magnitude less than **9**. Again, the NMR parameters for **8** and **9** (Tables 10 and 11) are very similar to those of **1** suggesting that **8**, **9**, and **1** adopt similar solution backbone conformations.

ROESY experiments were used to determine the chirality of the substituted Mamb C^{α}. The major difference between the data for **8** and **9** is the intensity of the ROE between the α-Ph-Mamb NH and the Asp H^{α} resonances (see Figure 9). The difference can be explained by assuming that the Mamb-Asp peptide bond will flip 180° to minimize the steric interaction between the Asp carbonyl oxygen and the Mamb α-phenyl group. The stronger Mamb NH-Asp H^{α} ROE observed in **8** is similar to the intensity seen in other peptides in this series. The weaker Mamb NH-Asp H^{α} ROE seen in **9** is consistent with a rotation of the Mamb-Asp peptide bond. Such a rotation would minimize the steric strain present in the L configuration.

From these data, we conclude that the α-Ph-Mamb is in the *R* configuration in **8**, while it is *S* in **9**. These results indicate that the chirality at the C^{α} of the Mamb determines the orientation of the Asp-Mamb amide group. In the *R* isomer the carbonyl group points up when viewed as in Figures 5–7 (top). This orientation matches the predominant conformation of **1**, and hence the compounds are equipotent. In contrast, the *S* isomer stabilizes the orientation in which the carbonyl points down and this compound is far less potent. Thus, it is probable that the predominant orientation of this amide carbonyl is retained during interaction with the IIb/IIIa receptor protein.

Crystal Structures of 1 and 2. Structural characterization of compounds **1** and **2** were carried out using standard X-ray crystallographic techniques. Several polymorphs of compound

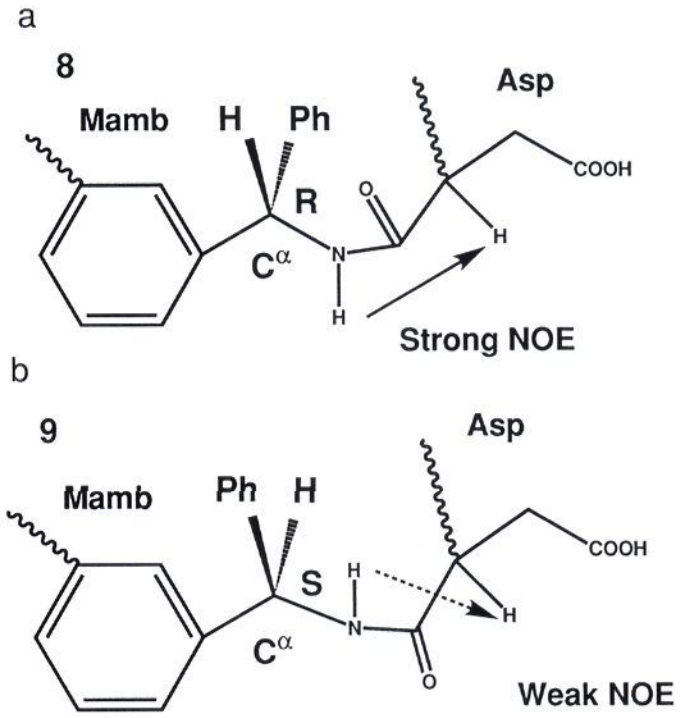

Figure 9. Summary of the key ROE observed in **8** (a) and **9** (a). From these data, **8** is assigned the *R* configuration and **9** the *S* configuration.

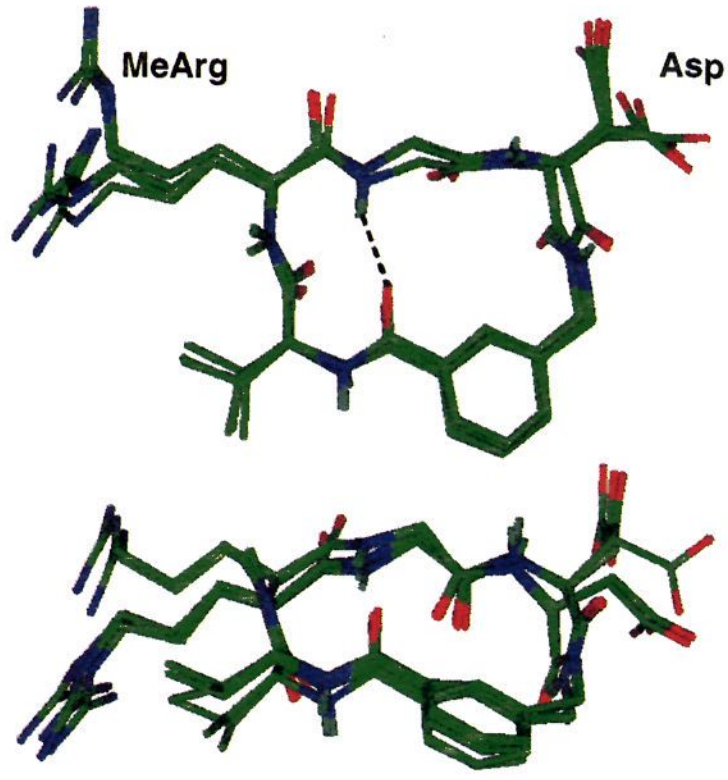

Figure 10. Overlay of the six crystal structures of **1** and **2**.

1 were completed to better determine its conformational flexibility in different crystalline environments. Recrystallization of zwitterionic **1** from water gave crystals of an orthorhombic polymorph, designated *1a*, whose asymmetric unit contained one peptide and approximately nine disordered water molecules.[7] From methanol, zwitterionic **1** gave primitive (*1b*) and C-centered (*1c*) monoclinic crystals; in both cases the solvent molecules, MeOH and H_2O, were disordered. The primitive form was noteworthy in that it contained two molecules of peptide per asymmetric unit. Recrystallized from water as the methyl sulfonate salt, compound **1** yielded orthorhombic crystals (*1d*) with a well-ordered asymmetric unit containing one peptide, one methyl sulfonate anion, and 3.5 molecules of water. The study of compound **2** was limited to one crystal, a structure in which the 12 water molecules of solvation were perfectly ordered.[41]

Comparison of the various crystal structures reveals a number of features worth mentioning. First, all of the studies (five structures and six peptide molecules) show that the macrocycles adopt very similar conformations as depicted in Figure 10. Second, all the rings have an intramolecular hydrogen bond (N41–H41N–O11) from the NH of Gly to the C=O of the Mamb moiety (see Figure 11). The persistence of this feature suggests that this hydrogen bond may help to limit the flexibility of the

(38) Janin, J.; Wodak, S. *J. Mol. Biol.* **1978**, *125*, 357–386.
(39) Ponder, J. W.; Richards, F. *J. Mol. Biol.* **1987**, *193*, 775–791.
(40) McGregor, M. J.; Islam, S. A.; Sternberg, M. J. E. *J. Mol. Biol.* **1987**, *198*, 295–310.

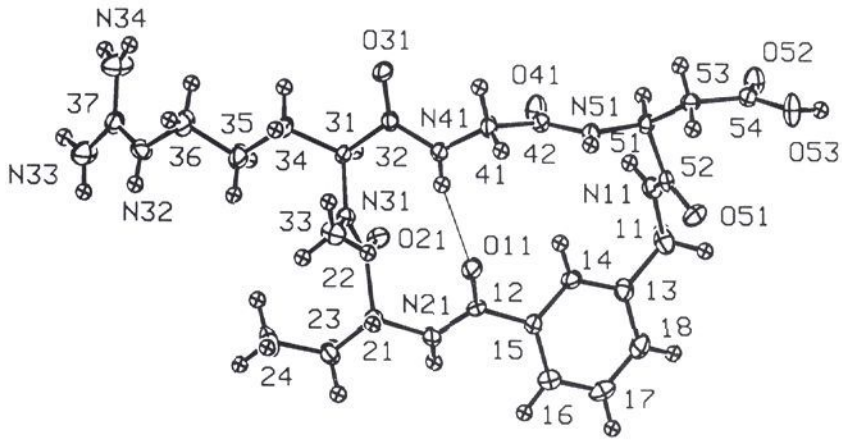

Figure 11. Peptide cation of compound *1d*, the methylsulfonate salt of **1**. Ellipsoids are drawn at the 50% probability level; hydrogen atoms have been assigned an arbitrary radius.

Table 13. ϕ and ψ Angles from the Crystal Structures of **1** and **2**

	X-Xxx		*N*-MeArg		Gly		Asp		
	ϕ	ψ	ϕ	ψ	ϕ	ψ	ϕ	ψ	quality[a]
1a	59.8	−135.4	−96.6	13.5	−83.0	−165.1	−73.6	−60.9	medium
1b	51.8	−135.7	−108.1	29.3	−109.2	−145.5	−98.0	97.6	low
	54.6	−139.6	−106.5	27.9	−106.6	−153.0	−93.2	100.9	
1c	49.0	−129.7	−111.5	31.3	−112.6	−153.3	−86.8	101.3	low
1d	55.1	−113.3	−107.4	36.1	−118.7	−144.0	−94.1	93.3	high
2	60.8	−130.0	−93.7	4.9	−80.3	−163.4	−82.0	−62.8	high
II′ β-turn	60	−120	−80	0					

[a] Quality of each structure is defined as follows. High: all atoms including solvent molecules and counter ions have been found and refined; non-hydrogen atoms with anisotropic thermal parameters, hydrogens with isotropic thermal parameters. *R* values less than 4%. Medium: peptide atoms found and refined with anisotropic thermal parameters; amide hydrogens refined but all others idealized. Water molecules disordered; refined occupancies and isotropic thermal parameters. *R* values in the 5–6% range. Low: peptide non-hydrogen atoms found and refined with isotropic thermal parameters; hydrogen atoms included in idealized positions. Solvent molecules (MeOH and H_2O) disordered; refined occupancies and anisotropic thermal parameters. *R* values range from 7.0–8.5%.

adjacent peptide backbone which includes D-Abu and *N*-MeArg groups. For example, note the consistency of the ϕ and ψ values for these groups in Table 13. The opposite side of the ring, however, is much more flexible with greater variation in the ϕ and ψ angles. Interestingly, the two amide bond orientations observed for the different diastereomeric C^{α}-phenyl Mamb analogues were both observed in the crystal structures of **1**. Combining the results for **1** and **2**, the predominant solution orientation was observed four times in the solid state and the other orientation was observed twice.

Another similarity among the five crystal structures relates to the nature of their packing: the peptide molecules in all five are found to align themselves in infinite chains, with each Arg "arm" reaching into the center of a neighboring peptide where the guanidinium cation forms multiple hydrogen bonds into the hydrophilic face of the peptide. Figure 12 contrasts the two faces of the cyclic peptide, one of which is lined with carbonyl oxygen atoms, the acceptors of the hydrogen bonds, while the other is largely hydrophobic in character. The similarity in the structures of the chains is remarkable (Figure 13) given that these materials include both neutral compounds and a salt, were grown from both H_2O and MeOH solutions, and crystallized in a variety of space groups. This uniformity strongly supports the concept of chain preassembly in the solution phase with crystallization occurring when the chains aggregate to create a three-dimensional lattice.[42,43]

Comparison of the X-ray Crystal Structure and the Solution Structures. As can be seen in Figure 14 and in comparing Tables 12 and 13, the NMR derived conformations are remarkably similar to those of the crystal structures. The most noticeable difference is that the Gly residue is not as fully extended in the crystal structure as in the NMR derived structures of **1**, **4**, and the extended conformational families of **5**. Secondly, the β-turns in the crystal structures are closer to ideal turn values.[44] Finally, a single value of χ_1, χ_2 for the side chain of the *N*-MeArg (−65°, 175°) was observed in the crystal structures, whereas two values (−180°, −180° and −50°, −180°) were observed in solution. The values in solution were limited by the lack of significant ROEs and the lack of dispersion in chemical shifts.

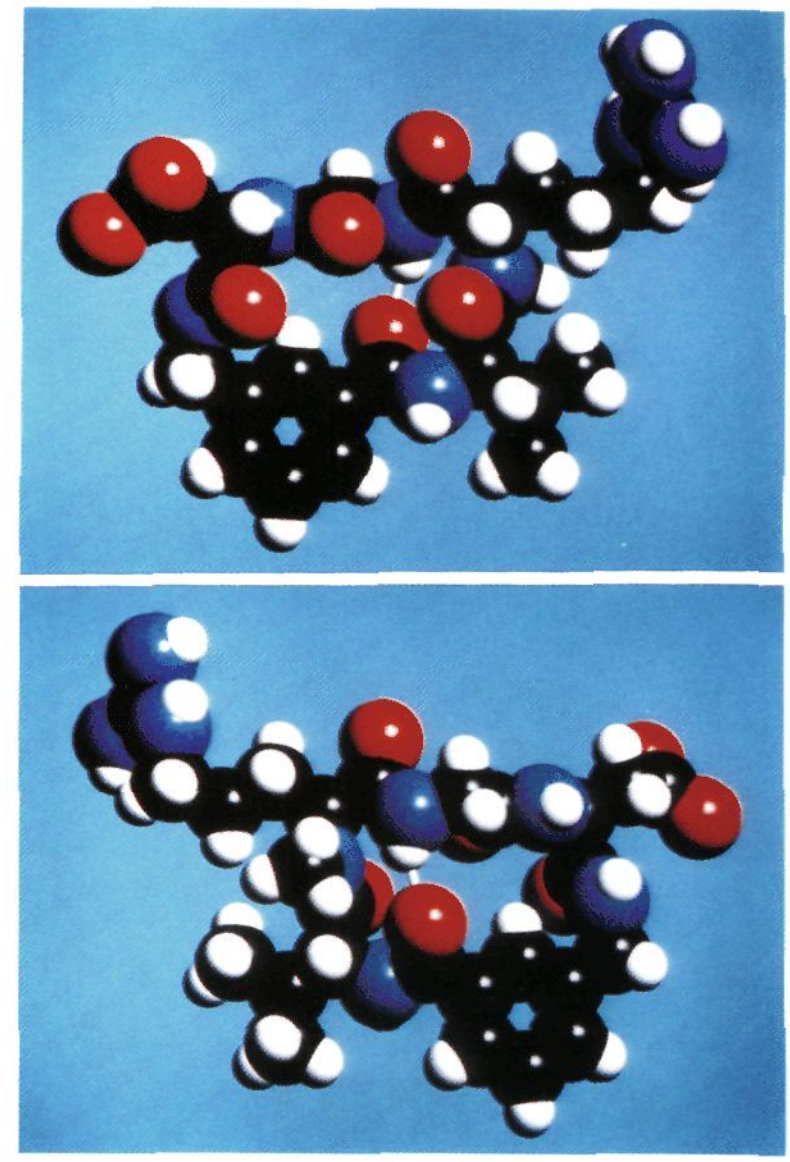

Figure 12. X-ray crystal structure of compound **2**. (a) Inside of the convex cyclic peptide showing its oxygen-rich character. (b) The other side of the peptide exhibits mainly hydrophobic groups.

Comparison to Other Cyclic RGD-Containing Peptides. Several other groups have recently reported the NMR-based conformational analysis of similar cyclic peptides with $GP^{IIb/IIIa}$ receptor antagonist activity. Bogusky *et al.* described two disulfide-linked cyclic pentapeptides, *cyclo*(Ac-Cys-Arg-Gly-Asp-Cys-OH)[30] and *cyclo*(Ac-Pen-Arg-Gly-Asp-Cys-OH).[45] Although no single conformation was found which described all the NMR data, they did find that the RGD portion was usually extended with the Gly residue in either the $i + 1$ or $i + 2$ position of a β-turn.

Kopple *et al.* reported two similar RGD compounds which adopted a turn-extended-turn conformation in methanol, (2-mercaptobenzoyl)-*N*-MeArg-Gly-Asp-2-mercaptoanilide cyclic disulfide, and Ac-Cys-*N*-MeArg-Gly-Asp-Pen-CONH2 cyclic disulfide.[23] In these compounds, the *N*-Me-Arg has ϕ, ψ angles similar to those for the $i + 2$ position of a β-turn. The Asp residue is at the $i + 1$ position of a γ-turn-like structure. Between these two residues is a highly extended Gly residue.[23] A more

(41) Harlow, R. J. *J. Am. Chem. Soc.* **1993**, *115*, 9838–9839.
(42) Hartman, P.; Perdok, W. G. *Acta Crystallogr.* **1955**, *8*, 49–52.
(43) Weber, P. In *Advances in Protein Chemistry*; Richards, F. M., Ed.; Academic Press: New York, 1991; pp 1–35.
(44) Rose, G. D.; Gierasch, L. M.; Smith, J. A. In *Advances in Protein Chemistry*; Anfinsen, C. B.; Edsall, J. T.; Richards, F. M.; Eds.; Academic Press: New York, 1985; pp 1–109.
(45) Bogusky, M. J.; Naylor, A. M.; Mertzman, M. E.; Pitzenberger, S. M.; Nutt, R. F.; Brady, S. F.; Colton, C. D.; Verber, D. F. *Biopolymers* **1993**, *33*, 1287–1297.

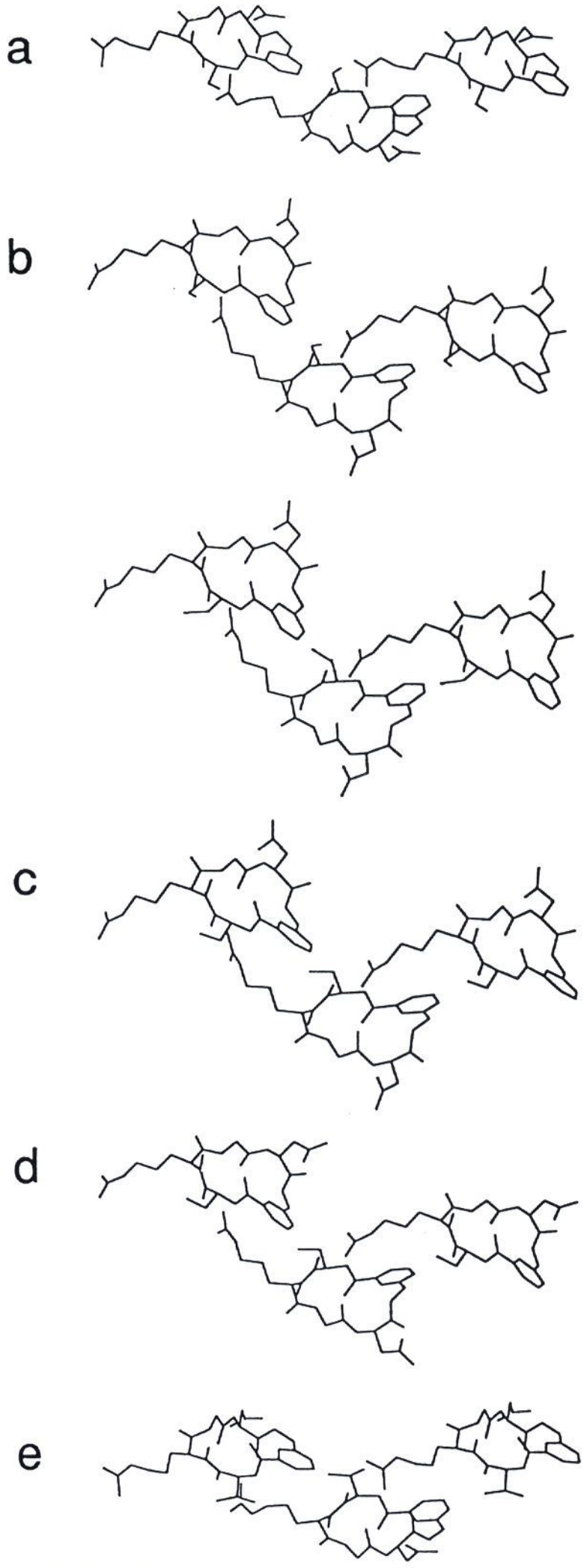

Figure 13. "Chain" packing of the molecules in the five crystal structures formed by the interaction of the guanidinium group of one molecule hydrogen bonding with the ring carbonyl groups of a neighboring molecule. The orientation of the center molecule in each case has been referenced with respect to the C31–C14 and N21–C42 vectors: (a) structure *1a*, space group $P2_12_12_1$; (b) *1b*, $P2_1$, with two molecules per asymmetric unit; (c) *1c*, C2; (d) *1d*, $P2_12_12$; (e) *2*, $P2_12_12_1$. Although not shown here, there is an expectation that aggregation would involve hydrogen bonds between the positively charged guanidinium moiety and the negatively charged Asp carboxylate anion, such direct pairing only occurs in the two crystals grown from MeOH (structures *1b* and *1c*). In water, a much more polar solvent, the packing produces no direct hydrogen bonding between these two charged groups (structures *1a* and *2*): instead, the interactions between the charged groups are mediated by water molecules.

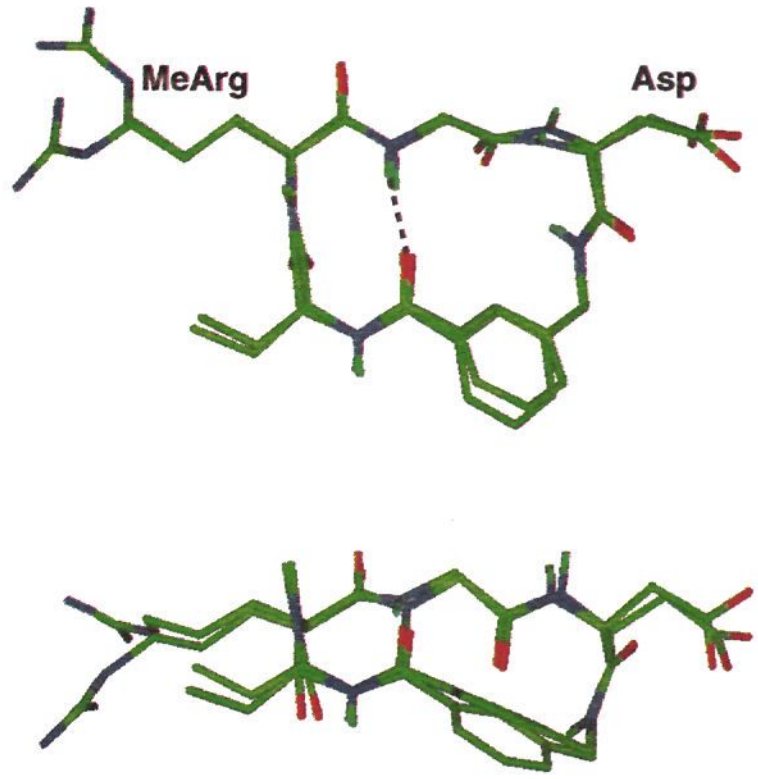

Figure 14. Overlay of the centroid conformer calculated for **1** and its X-ray crystal structure *1a*. The two conformations are extremely similar.

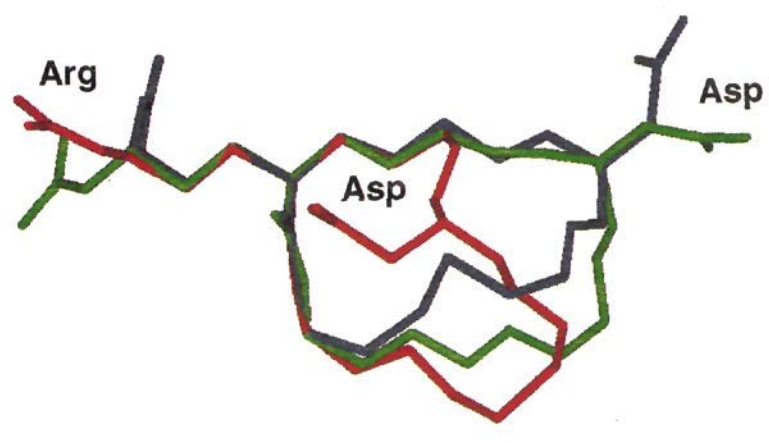

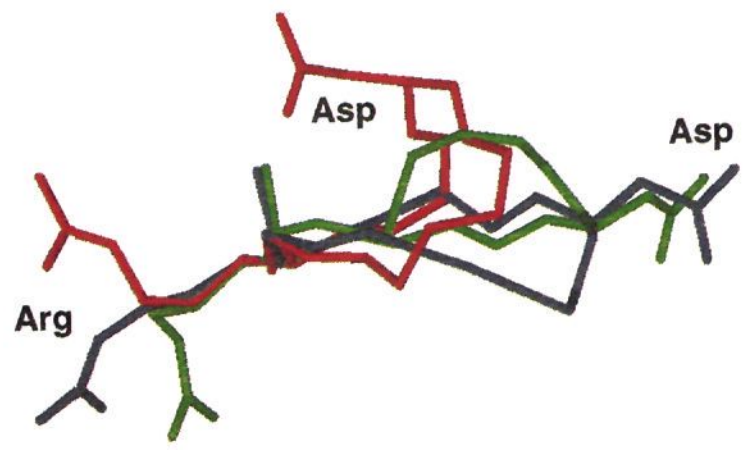

Figure 15. Overlay of (2-mercaptobenzoyl)-*N*-MeArg-Gly-Asp-2-mercaptoanilide cyclic disulfide from Kopple *et al.* (blue), *cyclo*(-Ac-D-Tyr-Arg-Gly-Asp-Cys-COOH from McDowell and Gadek (red), and the centroid conformation of **1** (green). Note there is good overlap for all three compounds at the β-turn region, but in the McDowell and Gadek compound the Asp residue bends up.

extensive study of related peptides has also been reported by Peishoff *et al.* which has verified the turn-extended-turn conformation as resulting in highly active compounds.[22]

The work presented in the present study is very consistent with these previous studies. The common features of an extended Gly residue and the turn-extended-turn motif are clearly similar.

Finally, McDowell and Gadek have reported the solution conformation of *cyclo*(D-Tyr-Arg-Gly-Asp-NH-CH(COOH)-CH_2-SO-CH_2-CO) in H_2O.[31] Analogous to compounds **1** and **4**, the D-Tyr-Arg dipeptide occupies positions $i + 1$ and $i + 2$ of a type II′ β-turn. However, the remainder of the structure is distinct

from **1**. This compound adopts what the authors call a cupped or bent conformation at the Gly residue.

In our work, we see this conformation in **5**, but we do not see any evidence for similar bent conformations in **1** or **4**. An overlay of **1** with the (2-mercaptobenzoyl)-*N*-MeArg-Gly-Asp-2-mercaptoanilide cyclic disulfide from Kopple *et al.*[23] and *cyclo*(D-Tyr-Arg-Gly-Asp-NH-CH(COOH)CH_2-SO-CH_2-CO) from McDowell and Gadek[31] (Figure 15) shows the different degrees of curvature from the bent backbone conformation of the McDowell and Gadek peptide, to the more extended Kopple *et al.* peptide, and finally to the slightly concave shape of **1** when viewed from the side.

Given the extreme potency of **1**, and its high affinity for IIb/IIIa, it is tempting to hypothesize that its predominant solution conformation is essentially identical to the active, receptor-bound conformation. However, it is difficult to reconcile these experimental facts with the finding that the McDowell and Gadek[31] compound shows a single conformation in solution but has a very different conformation in the Gly-Asp portion of the molecule. The McDowell and Gadek[31] compound is much less active than compound **1**, which would suggest that it might adopt a more extended conformation when bound to the receptor. Alternatively, **1** might adopt a receptor-bound conformation that is more bent at the Gly residue. In fact, unrestrained molecular dynamics calculations (without added solvent molecules) indicate that this compound is capable of adopting a more bent conformer (data not shown).

Conclusions

These studies represent an intensive set of experiments aimed at defining the conformation of cyclic RGD-containing peptides. The rigidity of **1** and **4** allowed the stereospecific assignment of the prochiral Gly protons, resulting in particularly high-quality solution structures. The great similarity in the six crystal structures of **1** and **2** further attest to the quality of the solution data as well as the rigidity of the peptide.

These results demonstrate the potential of the template constrained cyclic peptide approach for the design of conformationally restricted peptides. All nine of the peptides examined in this work adopt a β-turn at the first two positions of the sequence, indicating that the Mamb-containing macrocycle has effectively restricted the conformation of the intervening peptide sequence. The additional conformational constraints present in **1**—including an *N*-methyl group and a D-amino acid—further restrict the peptide to essentially a single conformer.

The results of this paper also help to explain why the D-Abu residue and *N*-methylation of the Arg in compound **1** give rise to such a potent compound. These modifications appear to preorganize the peptide into a conformation that is closely related to the receptor-bound conformer. Furthermore, an extended hydrophobic surface is created by the ethyl side chain of the D-Abu, the aliphatic portion of the Arg side chain, the *N*-methyl group of the *N*-MeArg, and the phenyl ring (Mamb); all of these groups segregate in one corner of the molecule. Presumably this hydrophobic surface is complementary to an apolar patch adjacent to the RGD-binding site of IIb/IIIa.

Acknowledgment. The crystal of *1d* was grown by A. L. Rockwell. The preliminary X-ray studies and data collections were performed by L. F. Lardear. We thank S. Jackson, J. A. Markwalder, and A. Parthasarathy for synthesizing the compounds described here.

Supplementary Material Available: Complete crystallographic reports for structures *1b*, *1c*, and *1d* including tables of atomic coordinates, thermal parameters, and interatomic distances and angles (30 pages). This material is contained in many libraries on microfiche, immediately follows this article in the microfilm version of the journal, and can be ordered from the ACS; see any current masthead page for ordering information.